Characterization and Uncertainty Analysis of a Reference Pressure Measurement System for Wind Tunnels

Tahani Amer, John Tripp, Ping Tcheng, Cecil Burkett, and Bradley Sealey
NASA Langley Research Center
Hampton, VA 23681

Abstract

This paper presents the calibration results and uncertainty analysis of a high-precision reference pressure measurement system currently used in wind tunnels at the NASA Langley Research Center (LaRC). Sensors, calibration standards, and measurement instruments are subject to errors due to aging, drift with time, environment effects, transportation, the mathematical model, the calibration experimental design, and other factors. Errors occur at every link in the chain of measurements and data reduction from the sensor to the final computed results. At each link of the chain, bias and precision uncertainties must be separately estimated for facility use, and are combined to produce overall calibration and prediction confidence intervals for the instrument, typically at a 95% confidence level.

The uncertainty analysis and calibration experimental designs used herein, based on techniques developed at LaRC, employ replicated experimental designs for efficiency, separate estimation of bias and precision uncertainties, and detection of significant parameter drift with time. Final results, including calibration confidence intervals and prediction intervals given as functions of the applied inputs, not as a fixed percentage of the full-scale value are presented.

System uncertainties are propagated beginning with the initial reference pressure standard, to the calibrated instrument as a working standard in the facility. Among the several parameters that can affect the overall results are operating temperature, atmospheric pressure, humidity, and facility vibration. Effects of factors such as initial zeroing and temperature are investigated. The effects of the identified parameters on system performance and accuracy are discussed.

Introduction

The development of advanced aircraft and improvement of present aircraft has placed stringent demands on wind tunnel facilities to improve productivity and data quality furnished to the customers. A wind tunnel testing improvement program at LaRC has been initiated. Among the objectives is an improvement of data quality to a level that meets national standards. Therefore, an assessment of the present measurement system uncertainties is required, followed by determination of needed improvements. The uncertainty of every parameter affecting the output of the measurement system must be determined to establish the overall system uncertainty. The most important factors affecting the uncertainty of a system are the accuracy of the individual instrument components, calibration procedures, human factors, environment, and reduction and analysis of test data. Moreover, the quality of the final results depends strongly on the type of experimental design selected for calibration (ref. 1). Batill has studied and identified sources of uncertainty at the National Transonic Facility (ref. 2).

Reference pressure is one of the most important measured parameters in any wind tunnel facility because it enters into the determination of several other core measurement calculations such as Mach number and aerodynamic coefficients. Therefore, a characterization of the reference pressure measurement system will provide insight to improve the measurement process.

Methodology developed by National Institute of Standards and Technology (NIST-1297) has been utilized to calibrate the high precision reference pressure transducer. In addition, the traceability chain for the transducer is developed in accordance with the procedures of reference 3.

Experimental Procedure

The reference pressure characterization project was conducted in three phases. In phase one, the identification process, a representative reference pressure instrument and a suitable wind tunnel facility were selected where experiments could be conducted under typical tunnel test conditions. In phase two, conducted by NIST & Wyle Laboratories, the instrument was calibrated under controlled environmental conditions. Finally, in phase three, the reference pressure measurement transducer was characterized in LaRC calibration laboratories (ref. 4).

Phase-One: Identification Process

All major wind tunnel facilities at LaRC were surveyed to identify the instruments used to measure reference pressure. The Ruska DDR6000 was selected for testing because it is used by most LaRC facilities for reference pressure measurement. The 0.3-Meter Transonic Cryogenic Tunnel was selected for facility testing because of system simplicity and ease of access.

Phase-Two: NIST & Wyle Laboratories Calibrations

The transducer was sent to NIST for calibration. Two complete calibrations were performed, on two different days, wherein the voltage outputs of the instrument were compared with readings of a NIST pressure standard (gas piston gage). The values of the applied pressure were corrected for environmental effects. The test results at NIST, taken over the two-day period, provided an overall value for uncertainty of U_{cal} = 0.00093 percent of full-scale output.

The transducer was later sent to Wyle Laboratories' local calibration laboratory to establish the accuracy of the transducer under normal laboratory conditions. The outputs produced by pressure applied over the range of the instrument were compared with the outputs of a secondary pressure standard. Corrections for temperature and gravitational effects were made. The total uncertainty was calculated as U_{cal} = 0.014 percent of reading plus 0.008 percent of full-scale. Results of the calibration at the local laboratory provided additional information to the calibration report to represent the total uncertainty of the instrument using the guidelines in reference 3.

Phase-Three: LaRC Characterization of the Reference Pressure Measurement Transducer

This experiment utilized calibration techniques and experimental designs developed and currently used at LaRC (ref. 5). The procedure included the following steps:

A) The calibration experimental design was established.
B) Calibrations were conducted with up to ten replications.
C) Calibration data was analyzed and results were presented graphically.
D) The most significant facility variable, operating temperature, was varied.
E) The effect of initial instrument zeroing versus numerical zeroing was evaluated.

Figure 1 depicts the experiment set-up and equipment used for the in-house calibration. The transducer was calibrated at different operating temperatures. Calibration tests disclosed that instrument zeroing does not affect its performance. Post-test numerical zeroing was equivalent to pre-test electrical zeroing. Data collection software was written in Quick Basic 4.5 for all data acquisition and instrument control.

Calibration, Experimental Design, and Uncertainty Analysis

The calibration procedures, experimental design, data analysis, and uncertainty analysis employed during the effort reported herein were developed at NASA LaRC and are documented in reference 5. In-house developed software was employed for all data analysis.

The pressure system calibration procedure employed a 21-point experimental design wherein ten equal-valued pressure loads are applied sequentially from zero, to full-scale, and back to zero. Six or more replications were conducted at each of three-fixed sensor temperatures. A second-order polynomial model is employed whose coefficients are determined by least-squares estimation. Calibration results are illustrated by means of residual plots augmented by calibration confidence interval and prediction interval curves presented as functions of the applied load, at a 95 percent confidence level.

It is shown in reference 5 that the calibration confidence interval and prediction interval are given by the following expressions:

$$|y - y| \le (\mathbf{z}^T \mathbf{Q}^{-1} \mathbf{z})^{1/2} \quad S_E \, t_{K-3-1} \, (\alpha/2)$$

where $y - y$ is the predicted output error at the specified confidence level, $\mathbf{Q}$ is the moment matrix of the calibration experimental design, $\mathbf{z}$ is the applied input vector, S_E is the standard error of the regression, t (α) is the 1 - α percentile of the t-distribution with K - 3 -1 degrees of freedom, and 1 - α is the desired confidence level, usually 0.95. The prediction interval for new input $\mathbf{z_0}$ is given by

$$|y - y| \le (\sigma_0^2 / \sigma_v^2 + \mathbf{z_0}^T \mathbf{Q}^{-1} \mathbf{z_0})^{1/2} \quad S_E \, t_{K-3-1} \, (\alpha/2)$$

where σ_0^2 is the new measurement error variance and σ_v^2 is the calibration measurement error variance.

As discussed in reference 5, replication, essential for instrument calibration, provides estimates of the precision uncertainty due to random errors and of the bias uncertainty due to unknown systematic errors. LaRC uncertainty analysis software quantifies overall calibration goodness of fit by the standard error of the regression, which is partitioned into the estimated bias standard error and precision standard error. The software furnishes a test of significance for the presence of bias error. Replication, to be conducted over a period of several weeks, also provides characterization of long-term stability and parameter drift. Accordingly, the LaRC software provides a test of significance for the presence of drift in linear sensitivity over the replicated calibration data.

Estimation of Calibration Parameters

The Ruska system was calibrated approximately 100 times. During calibration four data points were recorded at each pressure setting following a ten-second wait. Calibrations were performed at Ruska temperatures of 30º C, 36º C and 38º C (nominal) while the environmental (chamber) temperatures were set at 10º C, 24º C, and 35º C. A list summarizing the results of 46 selected calibrations is presented in Table 1. Columns listing file number, standard error of the regression, sensor temperature, and estimated linear sensitivity are shown for each calibration. The second-order coefficient, usually five to six orders of magnitude smaller than the linear term and therefore negligible, is not shown.

Data outliers were frequently encountered because of the aged pressure loading apparatus employed during calibration. Some of the data sets containing outliers are shown in the table. Note that the

standard error of the regression typically varies between 0.002% FS and 0.003% FS for data sets without outliers, compared to standard errors up to 0.007% FS for data sets with outliers.

Data Presentation

Figure 2 illustrates a typical residual plot of a single calibration of the system at 25º C chamber temperature and 30º C sensor temperature. Calibration confidence intervals and predication intervals at 95% confidence level are presented as continuous functions of the applied pressure, in contrast to the conventional practice where overall uncertainty is cited as a constant percentage of full-scale sensor output. The standard error of the regression, σ_v, is indicated in the figure. Note that estimated bias and precision errors shown on the figure are not applicable for single replications.

A systematic residual pattern is apparent during the first four loading points at 0, 5, 10, and 15 psi. This behavior, apparent in all calibration data sets, may be attributed to automatic gain switching internal to the pressure sensor electronics. In particular, the gain setting during the first four points, corresponding to sensor outputs less than 3 V, is lower during the next 13 points corresponding to inputs greater than 15 psi and outputs greater than 3 V. The same residual pattern was observed during use of a second higher precision voltmeter. Indeed, calibration of both voltmeters using a precision voltage standard disclosed neither the error pattern nor a gain shift at 3V. Consequently, it was concluded that the pressure system internal electronics are the source of the behavior. An alternative pressure sensor mathematical model using a piecewise polynomial fit over the two input ranges could be employed for improved accuracy if desired.

Replication

Figure 3 presents the calibration residual plot for nine replicated data sets, at 36º C nominal sensor temperature and 24º C chamber temperature, selected from data files p0414d through p0701d. Separate estimated bias and precision standard errors are shown. As discussed previously, the entire group of nine replications containing 189 observations was treated as a single data set for least-squares estimation of system parameters. Sensor temperature variation was controlled within 0.1º C in data files p0414d through p0625d; however, the temperature variation in file p0701d was 1.4º C.

A study was conducted of the variation of the standard error of the regression, estimated standard bias error, and estimated standard precision error, as the number of replication increases from one to nine. Figure 4 illustrates a plot of the three estimated errors versus replication number for the calibration data set of figure 2 taken at 36º C sensor temperature. It can be seen that all of the estimated errors become relatively stable following the fourth replication. Note further that bias uncertainty (≈ 0.0023% FS) dominates precision uncertainty (≈ 0.0014% FS). Inspection of the data discloses that bias uncertainty is due to the repeated error pattern caused by the system gain range shift at 15 psi. Random errors due to outliers are minimal occurring at 5 psi during the first replication only.

Figure 5 illustrates a curve of the standard error and estimated bias and precision errors versus replication number for the calibration data set of figure 3 taken at sensor temperature of 36º C. Here, the estimated standard error and precision error approach stability (at approximately 0.0044% FS and 0.0040% FS, respectively) only near the final replication because of the occurrence of frequent outlier points throughout the nine replications. Estimated bias error, on the other hand, stabilizes following the sixth replication at 0.0017% FS. Note also that the continued presence of outliers throughout the global data set causes precision uncertainty to dominate bias uncertainty, and it also produces larger overall estimated error values compared to the data set of figure 4.

Temperature Effects

Figure 6 illustrates a residual plot of a single calibration of the Ruska system at the nominal sensor temperature of 30º C. Note that the estimated standard error is 0.0094% FS, four times that shown in figure 2. Inspection of the data indicates that sensor temperature drifted downward 0.7º C during the calibration. This may explains the apparent hysteresis seen at zero psi input. Figure 7 presents the residual plot for the global regression on the set of five replicated calibrations at a nominal sensor temperature of 30º C. The standard error is 0.0186% FS, estimated bias error is 0.0104% FS, and the estimated precision error is 0.0155% FS. These errors are nearly an order of magnitude larger than the values shown for the replicated calibration of figure 3 at 36º C. As shown in figure 8 a total sensor temperature variation of 2.5º C was observed over the set of five replicated calibrations.

Figure 9 illustrates the residual plot of a single calibration at a nominal temperature of 36º C with a 1.4º C sensor temperature variation. The nominal test chamber temperature is 20º C with 8.3º C variation. This calibration was included among the nine replications in the data set processed figure 3. Note the modest 0.00261% FS standard error although data contained outliers on the return path and the 1.4º C sensor temperature variation during calibration. This value of standard error is approximately 30% higher than for data sets with sensor temperature controlled within 0.1º C. In the absence of additional test data, it appears that the system is more sensitive to sensor temperature variation at 30º C than at 36º C.

System Sensitivity

The ultimate purpose of the calibration process is to determine the system parameters, i.e., offset, linear sensitivity, and quadratic sensitivities, in addition to estimating system uncertainty. As mentioned previously, column four of table 1 lists the linear sensitivity for each calibration file. The mean sensitivity over all data sets shown in table 1 over three temperature ranges is 0.19980 V/psi. The maximum positive and negative variations in sensitivity about the mean are +0.00003 V/psi and -0.00003 V/psi, respectively, which corresponds to a maximum sensitivity variation of ±0.015% FS from 25° C to 38° C. Note that the manufacturer's specification lists the system precision at 0.003% FS over a specified temperature range of 18° C to 36° C.

Conclusions

In the absence of data outliers and with sensor temperature variation controlled to approximately 0.1º C, the standard error of a single replication is usually less than the manufacturer's quoted "precision" of 0.003% FS. However, the standard error of global replicated data sets typically exceeds 0.003% FS. This indicates that the long-term stability and parameter drift of the system do not meet the manufacturer's specification. The test data contained herein also indicate that sensor temperature variation should be controlled within ±0.1º C. It was found, as expected, that sensor electrical zeroing does not effect its performance. Post-test numerical zeroing was equivalent to pre-test electronic zero.

Acknowledgments

The authors wish to thank Richard Deloach for his contributions in the initial phase to identify the parameters to be considered for testing. In addition, the authors wish to thank James Walsh and Wyle Laboratories for supporting the calibration effort. Finally, input from the wind tunnel user's viewpoint by Michael Mitchell, James Hallissy, and Michael Hemsch is appreciated.

References

1. Box, George E. P., *Empirical Model-Building and Response Surfaces*, John Wiley & Sons, New York, NY, 1987.
2. Batill, Stephen M., "Experimental Uncertainty and Drag Measurements in the National Transonic Facility," NASA CR-4600, June 1994.
3. Taylor, Barry N., Kuyatt, and Chris E., "Guidelines for Evaluating and Expressing the Uncertainty of NIST Measurement Results," NIST-TN1297, 1994.
4. "Metrology-Calibration and Measurement Processes Guidelines," NASA RP 1342, June 1994.
5. Tripp, John S., and Tcheng, Ping, "Uncertainty Analysis of Instrument Calibration and Application," NASA TP, In publication, 1999.

Table 1. Ruska Pressure Sensor Calibration					
Data File	Standard Error	Sensor Temp	Sensitivity		Remarks
	% FS	ºC	V/psi		
tstcal0424	0.0024628	36.2	0.19979		
p0427d	0.0023789	36.0	0.19978		
p0429d	0.0020530	36.0	0.19979		
p0430d	0.0027710	35.9	0.19979		
p0501d	0.0023659	36.1	0.19980		
p0504d	0.0025953	35.9	0.19979		
p0504dd	0.0021257	35.9	0.19979		
p0505d	0.0024683	36.0	0.19977		
p0507d	0.0025569	36.0	0.19978		
p0514d	0.0023170	36.2	0.19977		
p0520d	0.0033559	36.6	0.19976		Outliers @ 40 psi
p0528d	0.0024624	36.5	0.19976		Outliers @ 35 psi
p0528e	0.0024132	36.5	0.19977		
p0601e	0.0016962	36.5	0.19977		
p0603d	0.0022078	36.4	0.19977		
p0623d	0.0021567	36.4	0.19981		
p0624d	0.0027448	36.3	0.19981		
p0624e	0.0024400	36.3	0.19980		
p0625d	0.0028540	36.4	0.19980		Outliers @ 20 psi
p0701d	0.0026056	35.7	0.19980		Outliers @ 15 psi & 1.4º C temperature drift
p0707d	0.0067432	36.0	0.19980		Outliers @ 10 psi
p0707e	0.0054321	36.0	0.19985		Outliers @ 50 psi
p0708d	0.0033150	36.0	0.19980		
p0709d	0.0024488	36.0	0.19981		
p0721d	0.0023991	35.9	0.19981		
p0721e	0.0025227	35.9	0.19980		
p0722d	0.0023991	35.9	0.19981		
p0722e	0.0025227	35.9	0.19980		
p0723d	0.0024488	36.0	0.19981		
p0723e	0.0024488	36.0	0.19981		
p0724d	0.0024020	36.0	0.19981		
p0724e	0.0022078	36.0	0.19977		
p0828d	0.0025238	35.5	0.19983		
p0831d	0.0021522	35.4	0.19982		
p0831e	0.0043839	35.4	0.19984		Outliers @ 35 psi
p0901d	0.0024694	35.4	0.19982		
p0902d	0.0051534	35.6	0.19987		Outliers @ 20 & 25 psi
p0902e	0.0046152	35.6	0.19982		Outliers @ 5 psi
p0911d	0.0049248	35.5	0.19985		Outliers @ 20 psi
p0915d	0.0027055	38.4	0.19980		Outliers @ 10 psi
p0916d	0.0021091	38.2	0.19980		
p0923d	0.0025854	38.2	0.19981		Outliers @ 10 psi
p0928d	0.0022116	38.2	0.19980		
p1007d	0.0025869	38.2	0.19981		Outliers @ 10 psi

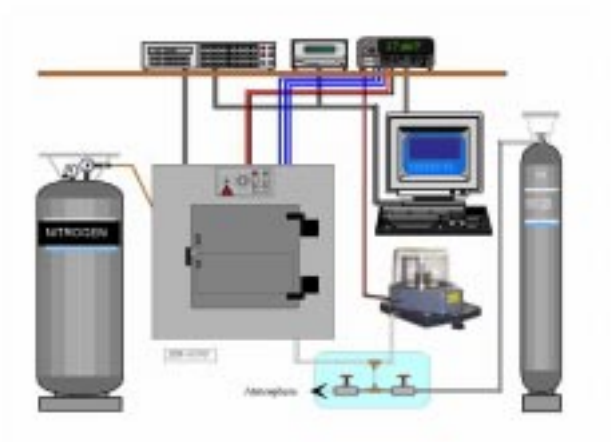

Figure 1. The experiment set-up for calibration of the sensor

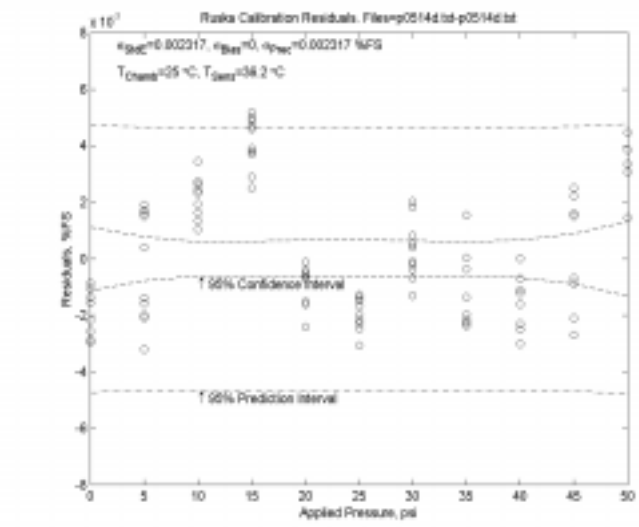

Figure 2. Typical residual plot of a single calibration at 25 °C chamber temperature

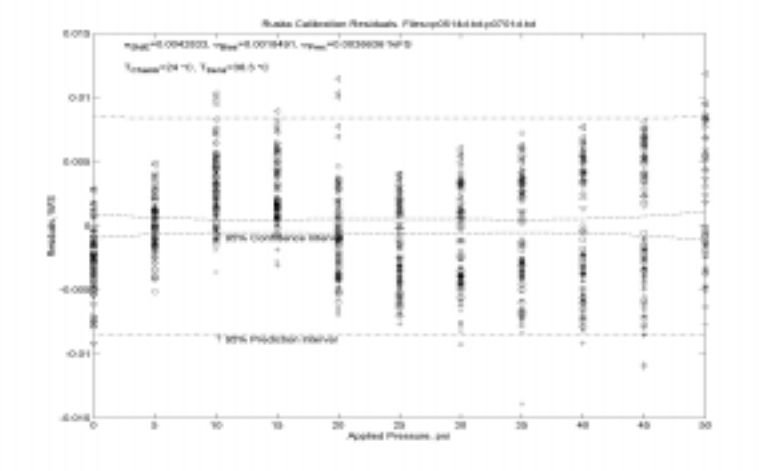

Figure 3. Residual plot of nine calibration replications at 24°C chamber temperature

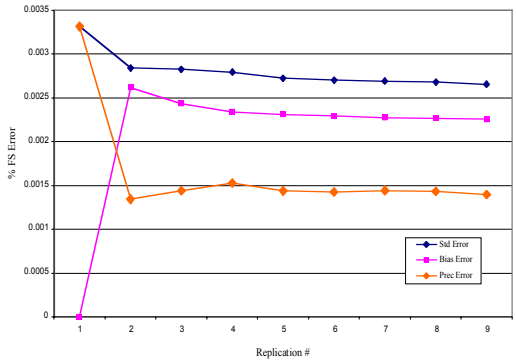

Figure 4. Plot of standard, bias, & precision estimated errors versus replication number at 24.5°C chamber temperature

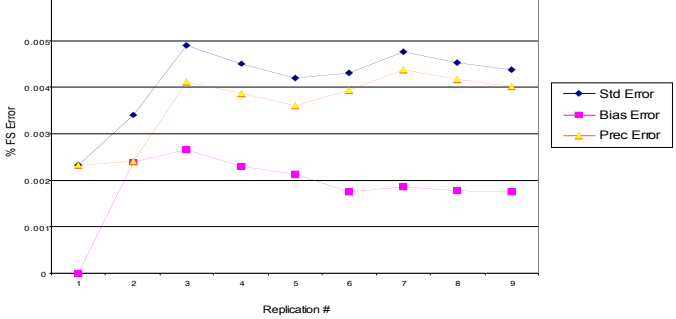

Figure 5. Plot of estimated standard, bias, & precision errors versus replication number at 36°C chamber temperature

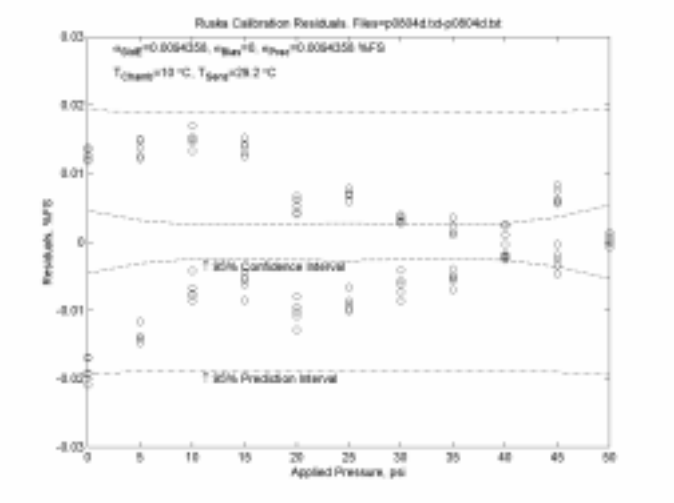

Figure 6. Typical residual plot of single replication at 10°C chamber temperature

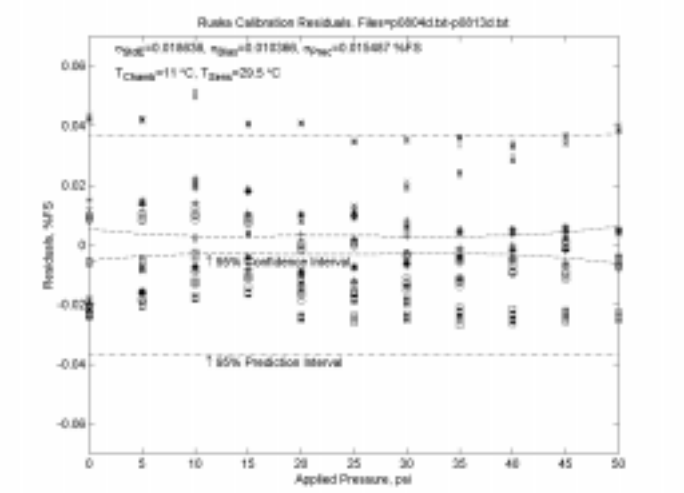

Figure 7. Residual plot for five replicated calibrations at 11°C chamber temperature

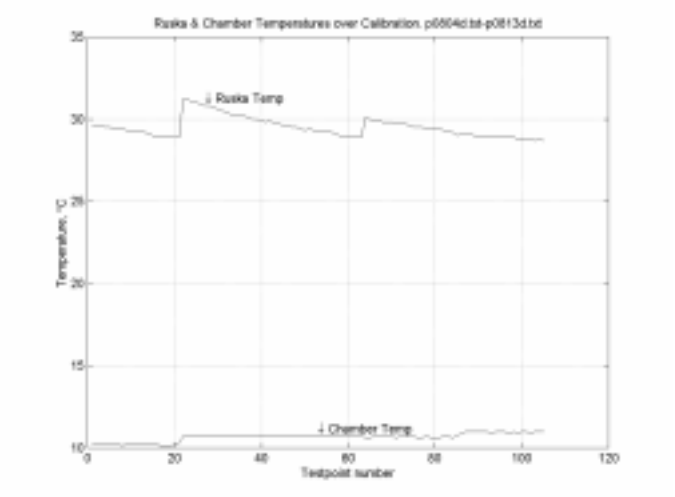

Figure 8. Sensor and chamber temperature history during nine replications (10° C nominal chamber temperature, 30° C nominal sensor temperature)

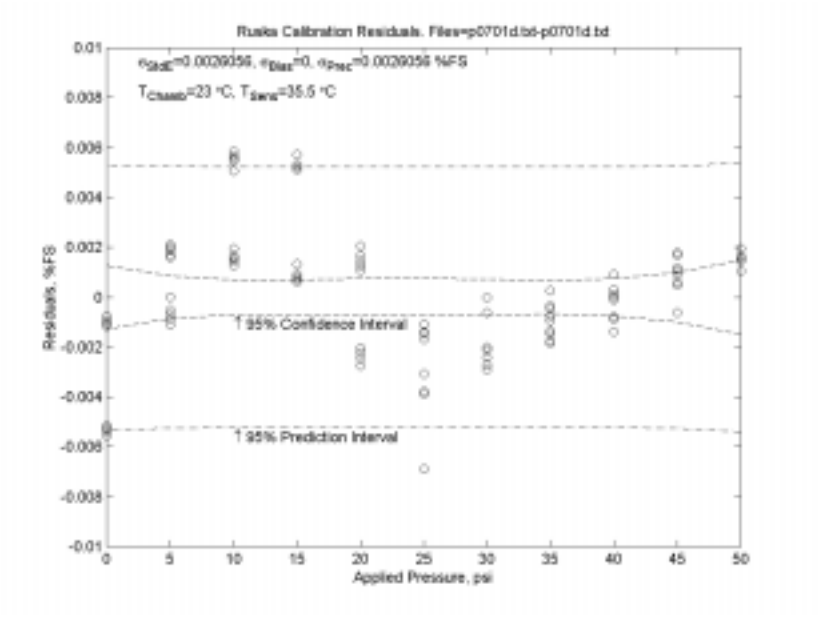

Figure 9. Residual plot of single calibration at 23 °C chamber temperature